Published in final edited form as:
J Mol Biol. 2007 January 5; 365(1): 196–210.

Fine and domain-level epitope mapping of botulinum neurotoxin type A neutralizing antibodies by yeast surface display

R. Levy[1], **C.M. Forsyth**[1], **S.L LaPorte**[1], **I.N. Geren**[1], **L.A. Smith**[2], and **J.D. Marks**[1,3]

1 *Department of Anesthesia and Pharmaceutical Chemistry, University of California, San Francisco Rm 3C-38, San Francisco General Hospital, 1001 Potrero Ave, San Francisco, CA 94110*

2 *Integrated Toxicology Division, United States Army Medical Institute of Infectious Diseases (USAMRIID), Fort Detrick, MD 21702*

Abstract

Botulinum neurotoxin (BoNT), the most poisonous substance known, causes naturally occurring human disease (botulism) and is one of the top six biothreat agents. Botulism is treated with polyclonal antibodies produced in horses which are associated with a high incidence of systemic reactions. Human monoclonal antibodies (mAbs) are under development as a safer therapy. Identifying neutralizing epitopes on BoNTs is an important step in generating neutralizing mAbs, and also has implications for vaccine development. Here we show that the three domains of BoNT serotype A (BoNT/A) can be displayed on the surface of yeast and used to epitope map six mAbs to the toxin domains they bind. The use of yeast obviates the need to express and purify each domain, and it should prove possible to display domains of other BoNT subtypes and serotypes for epitope mapping. Using a library of yeast displayed BoNT/A binding domain (H_C) mutants and selecting for loss of binding, the fine epitopes of three neutralizing BoNT/A mAbs were identified. Two mAbs bind the C-terminal subdomain of H_C, with one binding near the toxin sialoganglioside binding site. The most potently neutralizing mAb binds the N-terminal subdomain of H_C, in an area not previously thought to be functionally important. Modeling the epitopes shows how all three mAbs could bind BoNT/A simultaneously and may partially explain the dramatic synergy observed on in vivo toxin neutralization when these antibodies are combined. The results demonstrate how yeast display can be used for domain-level and fine mapping of conformational BoNT antibody epitopes and the mapping results identify three neutralizing BoNT/A epitopes.

Keywords

epitope mapping; yeast surface display; botulinum neurotoxin; affinity; alanine scanning mutagenesis

Introduction

Botulinum neurotoxin (BoNT) is secreted by the spore-forming bacteria *Clostridium botulinum* and is the most poisonous substance known [1]. The crystal structure of BoNT serotype A (BoNT/A) [2] shows three functional domains comprising a heavy and a light chain

[3]Corresponding author: Department of Anesthesia and Pharmaceutical Chemistry, University of California, San Francisco Rm 3C-38, San Francisco General Hospital, 1001 Potrero Ave, San Francisco, CA 94110 USA, tel: 415-206-3256, FAX: 415-206-3253, e-mail: marksj@anesthesia.ucsf.edu

[2-4]. The C-terminal portion of the heavy chain (H_C) is the binding domain which docks the toxin to sialoganglioside receptors and a protein receptor on presynaptic neurons, resulting in toxin endocytosis [5-7]. The translocation domain (H_N), at the N-terminal portion of the heavy chain, mediates escape of the toxin light chain (L_C) from the endosome. Depending on serotype, the L_C cleaves one or more members of the SNARE complex of proteins, blocking acetylcholine release [8, 9].

Human botulism is caused by BoNT serotypes A, B, E, and F and is characterized by flaccid paralysis which, if not fatal, requires prolonged hospitalization in an intensive care unit and mechanical ventilation. Naturally occurring botulism results from ingestion of contaminated food, anaerobic wound infections, or gastrointestinal tract colonization by Clostridial bacteria [10]. Botulinum neurotoxins are also classified by the Centers for Disease Control (CDC) as one of the six highest-risk threat agents for bioterrorism (the “Class A agents”) due to their extreme potency and lethality [11]. Both Iraq and the former Soviet Union produced BoNT for use as weapons [12, 13] and the Japanese cult Aum Shinrikyo attempted to use BoNT for bioterrorism [11]. Consequently, specific pharmaceutical agents are needed for treatment of intoxication.

Treatment of botulism in adults relies on the use of antitoxin [14], currently generated from immunized horses [15]. This product is associated with a high incidence of side effects, including serum sickness and anaphylactic shock. As an alternative, monoclonal antibody (mAb) based antitoxins are under development [16, 17]. Nowakowski and coworkers reported the generation of three mAbs, S25, C25, and 3D12, that neutralized BoNT/A both in vitro and in vivo [17]. While in vivo neutralization for single mAbs was of relatively low potency, combining any two or all three mAbs led to highly potent neutralization of BoNT/A. Higher affinity derivatives of these three mAbs are now in cGMP production for anticipated toxicology studies and human clinical trials (http://www3.niaid.nih.gov/news/newsreleases/2005/27million_bioshield.htm).

We have been interested in mapping the epitopes of these and other BoNT/A mAbs. Such mapping can lead to an improved understanding of mechanism(s) of toxin neutralization, as well as shed light on the relationship between toxin structure and function. For example, putative sialoganglioside binding sites on toxin have been identified using X-ray crystallography [18, 19]. Are these sites where neutralizing mAbs bind? Similarly, the BoNT/A docking site for the protein receptor remains unknown; identification of the epitopes for potently neutralizing BoNT/A mAbs might identify potential protein receptor binding sites on the BoNT/A H_C. Finally, marked synergy in toxin neutralization has been observed when mAbs are combined [17]. Identifying the sites and interactions between toxin and neutralizing mAbs could provide a structural model of the immune complexes and perhaps provide insights into mechanism of neutralization.

For this work, yeast display [20, 21] was utilized to successfully display all three BoNT/A domains, which could be used to map a panel of 6 mAbs to the domain level. This approach should prove useful for gross mapping of both polyclonal and monoclonal antibodies to BoNT/A and can probably be adapted for domains of other BoNT/A subtypes or other BoNT serotypes. This approach has an advantage of not requiring native protein expression and purification. Using yeast displayed libraries, the fine epitopes of neutralizing mAbs 3D12, HuC25, and S25 were identified down to the energetically important amino acid side chains. The results identify a number of neutralizing epitopes on BoNT/A and suggest mechanisms of toxin neutralization.

Results

Domain epitope mapping of BoNT/A neutralizing antibodies

To display the three functional domains of botulinum neurotoxin type A (BoNT/A H_C, H_N, and L_C) on the surface of yeast, we used PCR to amplify the relevant gene from plasmids containing either a synthetic H_C gene, or a synthetic L_C-H_N gene (Figure 1). PCR fragments encoding the H_C, L_C, H_N, and L_C-H_N were then ligated into the yeast display vector pYD2 [22] in frame with an SV5 epitope tag. This allowed for C-terminal fusion of the SV5 tag and a means to quantitatively measure the level of display on the yeast surface using a labeled SV5 mAb. Since Lacy and coworkers [2] previously described the presence of a ~50-residue belt (loop) region in the translocation domain that wraps around the L_C domain of BoNT/A, we designed an H_N variant which lacks the gene fragment that encodes for the belt region and also ligated this into pYD2. Ligation products were used to transform *E. coli*, clones containing the correct insert identified by DNA sequencing, and DNA prepared and used to transform *S. cervesiae*.

To demonstrate successful display of each of the BoNT/A domains, surface display was induced from each of the constructs and yeast co-stained with SV5 mAb labeled with Alexa-488 and BoNT/A specific mAbs labeled with Alexa-647. All five constructs (H_C, H_N with belt, H_N without belt, L_C, and H_N-L_C) were successfully displayed on the yeast surface as indicated by staining with SV5-488 (Figure 2a–e). To determine whether the displayed BoNT/A domains could be used to map monoclonal antibodies (mAbs), we studied a panel of BoNT/A mAbs previously shown to bind different toxin domains (Table 1). Both H_C-specific mAbs 3D12 23 and HuC25 [22] bound surface displayed H_C, but not H_N or L_C (Figure 2a). In contrast, the H_N specific mAb ING1 and the L_C-specific mAb ING2 did not bind surface displayed H_C (Figure 2a). Similarly, the L_C-specific mAb ING2 bound surface displayed L_C but did not bind H_C or H_N (Figure 2b). Surface displayed L_C was not bound by H_C or H_N mAbs (Figure 2b). Yeast surface displayed H_N domains (with or without the belt) were recognized by the H_N specific murine 9D8 mAb but were not recognized by H_C or L_C mAbs (Figure 2c, d). Surface displayed L_C-H_N was bound by both L_C (ING2) and H_N (9D8) mAbs, but not by H_C specific mAbs (Figure 2e). Finally, an interesting mAb (ING1) only bound surface displayed L_C-H_N, but did not bind displayed L_C or H_N. We had previously determined that this mAb bound recombinant L_C-H_N, but not L_C, and had assumed that it recognized an H_N epitope. The current results indicate that this mAb recognizes a complex epitope formed by the packing of the L_C and H_N, perhaps where the belt wraps around the L_C.

Fine epitope mapping of BoNT/A H_C-specific neutralizing monoclonal antibodies

To identify neutralizing epitopes on BoNT/A, we epitope mapped three neutralizing BoNT/A H_C mAbs (Table 1) down to the level of the energetically critical amino acid contacts between toxin and mAb. All three mAbs were initially single chain Fv (scFv) antibodies isolated from phage display libraries generated from immunized humans (3D12) or mice (S25 and C25) [16, 24]. The C25 antibody was subsequently humanized (HuC25), resulting in an antibody with a 2-fold higher affinity for BoNT/A than C25. After conversion to IgG with human Fc, all three mAbs showed in vitro BoNT/A neutralization, as evidenced by a prolongation in the time to paralysis in the hemidiaphragm assay, and in vivo neutralization, as evidenced by a prolongation in time to death in mice challenged with toxin (Table 1, and ref. [17]). For two of the mAbs, 3D12 and HuC25, fine epitope mapping was accomplished using an approach first described by Chao *et al.* [21] by: 1) generating a library of surface displayed BoNT/A H_C mutants; 2) selecting for loss of binding of the mAb being epitope mapped; 3) analyzing the location of mutations leading to loss of mAb binding; and 4) constructing single yeast displayed BoNT/A H_C alanine mutants in the putative mAb epitope and measuring the energetic contribution of the toxin side chain to mAb binding ($\Delta\Delta G$). For the third mAb, S25, we took

advantage of the fact that this mAb bound BoNT/A1 with high affinity but bound the BoNT/A2 subtype with much lower affinity [25]. Combining this fact with the knowledge that S25 bound the C-terminal subdomain of H_C, the H_{CC} of BoNT/A, a number of BoNT/A H_{CC} mutants were constructed substituting BoNT/A2 residues. The S25 epitope was identified based on loss of binding to a subset of the H_{CC} mutants.

Construction of a randomly mutated BoNT/A H_C library in yeast

To generate a library of BoNT/A H_C mutants, we utilized error prone PCR and amplification conditions known to introduce a high rate of mutations. Briefly, a high rate of mutations (~1.1% error-rate) was introduced into the BoNT/A H_C gene by amplification from the plasmid pYD2/H_C, using error prone PCR and conditions previously described by Fromant and coworkers [26]. The resulting gene repertoire was cloned into the yeast display vector pYD2 using gap repair homologous recombination to create a yeast library of ~ 3×10^5 transformants with an insert of the appropriate size, as determined by PCR screening. The library was grown, BoNT/A H_C epitope display induced and the library analyzed for display level by staining with SV5-Alexa-488, and mAb binding by costaining with 3D12-Alexa-647 and AR2-Alexa-647. AR2 is a higher affinity derivative of the HuC25 scFv [22]. A relatively low frequency of display (approximately 0.5%) and antigen binding (approximately 0.4 %) was observed, probably as a result of the high mutation rate (Figure 3).

Isolation of BoNT/A1 H_C clones with selective loss of binding to 3D12 or HuC25

To identify the epitopes recognized by 3D12 and HuC25, the epitope library was subjected to serial rounds of flow sorting. For the first round of sorting, H_C epitopes binding 3D12 and/or AR2 antibodies were recovered. This was accomplished by staining yeast with 3D12-Alexa-647, AR2-Alexa-647, and SV5-Alexa-488. Binding of 3D12 and AR2 mAbs to displayed H_C was detected using the APC (647nm) channel and binding of SV5 was detected using the FITC (488nm) channel. At this round, all Alexa-647 positive yeast were gated and sorted (Figure 3a). Co-staining with both 3D12 and AR2 labeled yeast functionally displaying either, or both, epitopes. The gate was set to include yeast with low to absent levels of SV5 display (SV5 binding), as these might represent clones with stop codons that contained the mAb epitope. Such clones would prove useful for narrowing the potential epitope space (see below). The library sort output was then grown, induced and subjected to a second round of selection that resulted in the recovery of only 3D12 (Alexa-647, gate P3) or AR2 (Alexa-488, gate P2) binding yeast clones (Figure 3b). This was accomplished by co-labeling the first round output with 3D12-Alexa-647 and AR2-Alexa-488. Two separate sort gates were set, one for Alexa-647 positive yeast and one for Alexa-488 positive yeast, and yeast collected separately for the two gates. Presumably at this round, loss of binding of one of the mAbs resulted from the presence of BoNT/A H_C mutations that resulted in minimal binding affinity for that mAb. Retained binding of the second mAb was utilized to ensure that the selected mutants were properly folded. Yeast from each sort gate were separately grown, induced and used for the next round of sorting.

For the final round of sorting, yeast from each of the previous two gates were stained in separate reactions with 3D12-Alexa-647, AR2-Alexa-488 and unlabeled SV5 mAb followed by anti-mouse-PE, to allow separate quantitation of the display level. For selection of well displayed epitopes bound only by mAb 3D12 (putative AR2/HuC25 epitopes), sort gates were set to include the 3D12-Alexa-647 positive population (APC positive) (sort gate P4, top panel, Figure 3c) and the AR2-Alexa-488 negative population (FITC negative) (sort gate P3, top panel, Figure 3c). These gates were set to include only the PE positive population, representing those yeast with positive SV5 binding (well displayed BoNT/A H_C). The P3 and P4 gates were intersected and only yeast in both gates collected. A separate sort gate (P2, top panel, Figure 3c) was set to collect potential poorly expressed AR2/HuC25 epitopes bound by 3D12-

Alexa-647 (APC positive and PE negative). Since this population was not bound by AR2-Alexa-488 (top left panel, Figure 3c), this gate was directly collected without the need for intersection. For selection of well displayed epitopes bound only by mAb AR2 (putative 3D12 epitopes), sort gates were set to include the AR2-Alexa-488 positive population (FITC positive) (sort gate P4, bottom panel, Figure 3c) and the 3D12-Alexa-647 negative population (APC negative) (sort gate P5, bottom left panel, Figure 3c). These gates were set to include only the PE positive population, representing those yeast with positive SV5 binding (well displayed BoNT/A H_C). The P4 and P5 gates were intersected and only yeast in both gates collected. A separate sort gate (P2, bottom panel, Figure 3c) was set to collect potential poorly expressed 3D12 epitopes bound by AR2-Alexa-488 (APC positive and PE negative). Since this population was not bound by 3D12-Alexa-647 (bottom panel, Figure 3c), this gate was directly collected without the need for intersection.

Identification of the 3D12 and HuC25 epitopes

To identify the 3D12 and HuC25 epitopes, 50 individual yeast clones from the sort output of the last round of selections by flow cytometry were grown in liquid culture and BoNT/A H_C display induced. Induced yeast cells were then incubated with HuC25 or 3D12 mAbs and binding quantitated by flow cytometry following incubation with APC-conjugated goat-anti-human $F_{(AB)'2}$ and anti-SV5 (Alexa-488). The H_C gene fragments from clones that were able to bind exclusively to 3D12 or HuC25 were amplified by PCR and the H_C gene sequenced. DNA sequencing revealed multiple different H_C mutants from each sorting, with each mutant containing between 3 and 15 different mutations. Molecular modeling of the locations of mutations on the X-ray crystal structure of BoNT/A enabled the selection of individual H_C amino acid residues that could potentially form the 3D12 (mutations from clones that could only recognize HuC25) or the HuC25 (mutations from clones that could only recognize 3D12) functional epitopes. Of great assistance in identification of the HuC25 and 3D12 epitopes were clones sequenced from the sorts where there was no SV5 tag expression. A number of different mutants containing stop codons were identified which bound HuC25, but did not bind 3D12 or anti-SV5. The most C-terminal of these was at amino acid position 1101, demonstrating that the 3D12 epitope was distal to this amino acid in the H_{CC} subdomain of BoNT/A H_C. Conversely, since HuC25 bound the clone with the stop codon at this position, the HuC25 epitope must be proximal to this amino acid, in the H_{CN} subdomain of the BoNT/A H_C. To confirm this assumption, yeast displaying either the H_{CC} (amino acid residues 1093 to 1296) or the H_{CN} subdomain (amino acid residues 876 to 1092) were generated by PCR amplification from pYD2/H_C. Induced yeast displaying H_{CN} bound HuC25 but not 3D12 and yeast displaying H_{CC} bound 3D12 but not HuC25, confirming the epitope location based on sequencing. Location of the epitopes to the subdomains allowed elimination of approximately half of the mutations from consideration.

Analysis of the location of mutations from selected clones resulted in the identification of a single loop of the H_{CC} (residues 1127 to 1131, Table 2), which had substitutions in all clones sequenced that had lost binding to 3D12. To confirm this site as the functional epitope for 3D12, six single alanine mutants were made for each of these residues. Truncation of the amino acid side chain to alanine allows quantitation of the energetic contribution of that residue to binding [27, 28]. Alanine substitutions were generated by a) PCR amplification of H_C using primers that introduced the alanine mutations, and b) homologous recombination of the resulting PCR products by gap repair to yield the final pYD2/H_C (alanine substituted) plasmids in yeast (Figure 4). 3D12 F_{AB} was used to determine the impact of alanine mutations on antibody binding affinity and energetics to avoid bivalent binding of the two F_{AB} heads of the IgG to the multiple copies of yeast displayed H_C, which could lead to an avidity effect and an overestimation of the binding constant [29]. The relative binding of the yeast displayed H_C alanine mutants to K_D concentrations of 3D12 or HuC25 F_{AB} was analyzed by flow cytometry

using APC-F_{AB}-specific antisera and SV5-Alexa-488 labeled antibodies (Table 2 and Figure 5). Three mutations (G1129A, I1130A and R1131A) virtually eliminated binding of 3D12 F_{AB} while binding of HuC25 F_{AB} was unchanged (Table 2, Figure 5b). Confirming the relative binding results, the K_D for binding of 3D12 F_{AB} to G1129A, I1130A and R1131A was 7.3 nM to 18 μM, a 45 to more than 100,000 fold reduction in affinity compared to the wildtype affinity of 3D12 for BoNT/A H_C (Table 3). Modeling of the location of the amino acids in the functional epitope of 3D12 on the BoNT/A crystal structure shows that 3D12 binds at the periphery of the BoNT/A H_{CC} (Figure 6b). The 3D12 functional epitope spans a single loop with a compact and well defined lobe which protrudes outwards from the H_C surface, the centermost residue of which is R1131. While this epitope may appear linear, binding of 3D12 F_{AB} to yeast displayed BoNT/A H_C could not be competed with a 19mer peptide epitope (data not shown).

Identification of the HuC25 epitope was less straightforward. Analysis of the location of mutations reducing or eliminating binding to HuC25 suggested 4 different loops for evaluation (β25, β27, and β35, and β 36) [30]. As a result, a much larger number of alanine mutants (27) were generated and analyzed compared to the 3D12 epitope (Table 2 and Figure 5a). Nine of the mutants (N918A, L919A, E920A, F953A, R1061A, D1062A, T1063A, H1064A, Y1066A) resulted in a significant reduction in binding of H_C to HuC25 revealing that the epitope spanned four loops of the H_C (β25, β27, β35, and β36 (Tables 2 and 3 and Figure 5a)). The most energetically important residues were F953 and H1064 (Table 3). Modeling of the location of the amino acids in the functional epitope of HuC25 on the BoNT/A crystal structure shows that HuC25 binds to the BoNT/A H_{CN}, near the interface with H_{CC} (Figure 6c). Unlike the 3D12 epitope, the HuC25 functional epitope is more discontinuous, spans a larger surface area on H_C, and includes amino acid residues located in four distinct turns (N918, L919, E920 in one turn, F953 in a second turn, R1061, D1062, T1063, H1064 in a third turn and Y1066 in a fourth turn).

Identifying the epitope of S25

To identify the epitope of S25, we first measured binding to BoNT/A H_{CN} and H_{CC} and determined that S25 bound H_{CC}. We then took advantage of the fact that S25 bound BoNT/A1 with high affinity but barely bound the BoNT/A2 subtype [25]. Amino acid differences between BoNT/A1 and A2 H_{CC} were identified and four yeast displayed BoNT/A mutants constructed with BoNT/A2 substitutions inserted as residues 1117, 1254-56, 1271-74, or 1294-95. Only the mutant 1254-56 showed loss of binding to S25, while retaining wildtype binding to 3D12. Modeling of the location of these amino acids on the BoNT/A crystal structure shows that S25 binds to the BoNT/A H_{CC} very near the putative sialoganglioside binding site (Figure 6a) [31].

Modeling the interactions of C25, 3D12, and S25 with BoNT/A

We previously showed that a combination of C25, 3D12, and S25 IgG neutralized BoNT/A in vivo with markedly greater potency than either the single mAbs or mAb pairs [17]. Molecular modeling based on the mAb epitopes indicates that all three mAbs can bind BoNT/A simultaneously confirming biophysical studies (Figure 7). The two mAbs which bind the BoNT/A H_{CC} overlap the putative sialoganglioside binding site and cover a large portion of H_{CC}, the domain thought to be more important for interaction with cellular receptors [31-33]. C25 (HuC25) binds the H_{CN}, near the interface with H_{CC}. Recent data suggests that antibodies to regions around this interface are important for toxin neutralization [32]. C25 is the most potently neutralizing mAb described [17], its epitope is near the H_{CN}-H_{CC} interface, and its epitope could represent a putative binding site for the recently identified BoNT/A protein receptors SV2 [5, 7]. The model of multiple mAb binding illustrates how a large portion of the toxin binding domain is occupied in regions known to be functionally important. This surface

blockade, combined with a known synergistic effect on affinity of binding [17], may partially explain how these mAbs synergize to neutralize BoNT/A.

Discussion

The three functional domains of BoNT/A were successfully displayed on the surface of yeast allowing the domain epitope mapping of a panel of six monoclonal antibodies. It was also possible to display a pair of domains (H_N-L_C, 100kDa), the largest protein displayed on the surface of yeast [21]. At least three of these mAbs (HuC25, 3D12, and S25) are known to bind conformational epitopes on the H_C [23]. One of the BoNT/A mAbs studied (ING1) bound H_N-L_C, but did not bind H_N or L_C. A potential epitope for this mAb would be the belt as it wraps around the L_C or a conformational epitope at the interface of the H_N-L_C. These results suggest that the domains are not only displayed, but properly folded. The affinities measured for mAb binding to yeast displayed domains were nearly identical to the affinities measured for pure neurotoxin. This is additional evidence that the domains are properly folded. Since the seven BoNT serotypes (A–G) share the same structural folds, it is likely that many, or all, domains of other BoNT serotypes could be successfully displayed on yeast. For example, we have been able to display at high level all three domains of BoNT serotype B (R. Levy and J.D. Marks, unpublished data). Display of BoNT domains of other serotypes would facilitate mAb domain epitope mapping and the measurement of binding affinity without the need to produce or purchase BoNT, which is a select agent and subject to the regulations governing its possession. In addition, at least 18 subtypes exist for the seven BoNT serotypes [25]. These subtypes differ between each other by 2.6 to 31.6 % at the amino acid level, and these differences can result in differential mAb binding [25]. It should also prove possible to generate yeast displayed subtype domains, which could be used to confirm mAb binding and measure the binding affinity, again without the need to express and purify each of the toxin subtypes.

It also proved possible to fine epitope map three H_C mAbs down to the energetically important toxin amino acids. Many methods have been employed in the past to map antibody binding epitopes using either linear peptides on pins or spotted on cellulose membranes [34], peptide fragments expressed in *E. coli* [35], yeast [36], or bacteriophage display libraries [23, 37, 38]. Such approaches are limited to mAbs binding either linear epitopes, or epitopes not requiring fully folded and full length conformationally correct domains. For example, neither 3D12, C25, nor S25 bind linear 15mer peptide epitopes and do not recognize Western blotted BoNT/A [23]. Selecting a library of BoNT/A H_C fragments displayed on phage resulted in only the C-terminal subdomain of H_C (H_{CC}) being selected for the S25 and 3D12 epitopes and C25 only selected full length H_C 23. Thus, while potentially narrowing the epitope space, such approaches are not useful for the fine mapping of mAbs recognizing conformational epitopes.

One approach for precise identification of conformational protein epitopes is alanine scanning, constructing individual alanine mutants of each residue, expressing and purifying protein, and measuring the binding affinity [27]. Recently, shotgun scanning mutagenesis has been described, a high throughput method for mapping paratopes and protein-protein interactions using phage display [39, 40]. In this approach, the relative functional impact of each amino acid is determined by the relative frequency of alanine mutants vs wildtype. Precise quantitation of $\Delta\Delta G$ requires expression and purification of each alanine mutant. More recently, it has proven possible to identify conformational antibody epitopes of complex proteins from yeast displayed libraries, including epitopes on EGF receptor and West Nile envelope protein [21, 41]. Like Oliphant *et al*, two mAbs binding non-overlapping conformational epitopes were utilized in this work for selection of loss of binding mutations. Retention of binding of the second mAb ensured that mutants were selected on the basis of mutations in the epitope, rather than selection of unfolded or poorly displayed mutants. The method was refined by also staining for SV5 epitope tag expression, as well as the binding of two mAbs. This allowed separation of well expressed

mutants from mutants with C-terminal truncations due to the random insertion of stop codons. Analysis of such mutants helped identify the minimal binding fragment and allowed simplification of mutant analysis.

The results of mAb epitope mapping sheds further light on BoNT/A structure and function, the location of neutralizing epitopes, and mechanisms of mAb synergy in toxin neutralization. All three mAbs studied neutralize BoNT/A *in vitro* as evidenced by a prolongation in time to neuroparalysis in the hemidiaphragm assay and inhibition of cellular cleavage of the catalytic domain substrate SNAP-25 [16, 17, 24, 42]. As these mAbs all bind the toxin binding domain, neutralization is likely to occur via blockade of cellular binding and uptake. S25 blocks BoNT/A binding to gt1b sialoganglioside immobilized in a BIAcore (B. Yowler, unpublished data) and its epitope maps closely to the gt1b binding site on H_{CC}. 3D12 also maps to H_{CC} and along with S25 covers a large portion of H_{CC}, the domain thought to be important for interaction with cellular receptors [31-33]. C25 (HuC25) binds the H_{CN}, near the interface with H_{CC} in a neutralizing region [32] that could represent a putative binding site for the recently identified BoNT/A protein receptors SV2 [5, 7]. Our model of multiple mAb binding illustrates how a large portion of the toxin binding domain is occupied in regions known to be functionally important. This surface blockade, combined with a known synergistic effect on affinity of binding [17], may partially explain how these mAbs synergize to neutralize BoNT/A. The proximity of the three mAb Fc domains are also available for interaction with Fc receptors which could enhance toxin clearance from the circulation [43].

Materials and Methods

Strains, media and antibodies

The yeast strain EBY100Zeo was a gift from Dr. Feldhaus (Pacific Northwest National laboratory, Richland, WA). Briefly, EBY100Zeo was derived from EBY100 (GAL1-AGA1:URA3 ura3-52 trp1 leu2*Δ1 his3Δ200 pep4::HIS2 prb1Δ1.6R can1 GAL*) and carries the pTEF1 promoter Zeocin resistance gene (Sh *ble* gene). EBY100Zeo was maintained in YPD media (*Current Protocols in Molecular Biology*, John Wiley and Sons, Chapter 13.1.2). The bacterial strain *E. coli* DH5α, (K12,Δ(*lac-pro*), *sup*E, thi, *hsd*D5/F′ *tra*D36, *pro*A+B+, *lac*Iq, *lac*ZΔM15) was used for cloning and preparation of plasmid DNA. The gene fragment encoding for botulinum neurotoxin type A (Hall) (BoNT/A) binding domain (H_C) and the expression plasmid pET24a/(L_C-H_N) harboring the gene fragment that encodes for the fusion of light chain (L_C) and translocation domains (H_N) of BoNT/A were kindly provided by Dr. Leonard Smith (USAMRIID, MD)[44-48]. LiAc–treated EBY100Zeo cells were transformed, as previously described [49], with plasmid derivatives of the pYD2 yeast display vector (see below) and selected on SD-CAA medium (*Current Protocols in Molecular Biology*, John Wiley and Sons, Chapter 13.1.2). H_C yeast surface display was induced by transferring yeast cultures from SD-CAA to SG-CAA medium (identical to SD-CAA medium except the glucose was replaced by galactose) supplemented with 12.5 μg ml^{-1} tetracycline, 50 μg ml^{-1} kanamycin and 25 μg ml^{-1} zeocin and growing at 18°C for 48 h, as described [50].

BoNT/A neutralizing monoclonal antibodies (mAbs) 3D12, HuC25, AR2, ING2, ING1, 9D8, and S25 were used [17, 22, 25]. For IgG and F_{AB} fragment detection by flow cytometry (FACS), Phycoerythrin (PE)-labeled goat-anti-human IgG, PE-labeled goat-anti-mouse IgG or F_{AB}-specific Allophycocyanin (APC-647nm)-conjugated goat anti-human $F_{(AB')2}$ were employed (Jackson ImmunoResearch Laboratories, PA). Expression in yeast was monitored using an SV5 antibody that was purified from hybridoma supernatant with a Protein G column (GE Healthcare, NJ) and then directly labeled with Alexa-488 or Alexa-647 with a kit provided by Molecular Probes (Carlsbad, CA).

Oligonucleotide primers

The following oligonucleotides were purchased from Sigma-Proligo (St. Louis, MO):

HCFor: 5′-ATATAAACACCATGGCCACCTCCATCCTGAACCTGCGC-3′

HCRev: 5′-TAGTATATATGCGGCCGCCAGCGGACGTTCACCCCAACC-3′

LCHnFor: 5′-ATATATAATCCATGGTTCAGTTCG TTAACAAACAGTTCAACTAC-3′

LCRev: 5′-TGTATAATTGCGGCCGCTTTGTTGTAACCTTTGTCCAGAGATTTAG-3′

LCHnRev: 5′-TGTATAATTGCGGCCGCCTGGTTGTCAACGTATTTGGACAGC-3′

HNBeltFor: 5′-ATATATAATCCATGGCTCTGAACGACCTGTGCATCAAAGTTAAC-3′

HCFor: 5′-ATATATAATCCATGGCACTGGACAAATACACCATGTTCCACTACC-3′

LCFor: 5′-CGTGTTTTCAAAGTTAACACTAACG-3′

Gap5: 5′-TTAAGCTTCTGCAGGCTAGTG-3′

Gap3: 5′-GAGACCGAGGAGAGGGTTAGG-3′

PYDFor: 5′-AGTAACGTTTGTCAGTAATTGC-3′

GAP3Rev: 5′-GAGACCGAGGAGAGGGTTAGG-3′

GAP31Rev: 5′-GAGAGGGTTAGGGATAGG-3′

Construction and expression of plasmids for yeast display of BoNT/A domains

The yeast display vector pYD2 was derived from pYD1 (Invitrogen, Carlsbad, CA), as previously described [22]. Primers HCFor and HCRev were designed to PCR amplify the H_C gene fragment, adding the restriction sites *NcoI* and *NotI*. The resulting PCR product and pYD2 were then both digested with *NcoI* and *NotI* and their ligation resulted in the yeast display vector pYD2/H_C. Primers LCHnFor and LCRev were designed to PCR amplify the L_C gene fragment from the expression vector pET24a/(L_C-H_N), adding the restriction sites *NcoI* and *NotI*. Following digestion of both pYD2 and the resulting PCR amplification product with *NcoI* and *NotI*, L_C was gel-purified and ligated into pYD2 to yield the yeast display vector pYD2/L_C. Similarly, reverse primer LCHnRev and forward primers HNBeltFor or HCFor were used in order to PCR amplify the gene fragments encoding for the translocation domain H_N with or without the belt region, respectively. Subsequently, ligation into pYD2 yielded the yeast display vectors pYD2/H_N (including the belt) and pYD2/H_N (without the belt). In order to construct the plasmid pYD2/L_C-H_N, primers LCFor and LCHnRev were first used to PCR amplify a C-terminal portion of L_C-H_N from plasmid pET24a/L_C-H_N adding the restriction sites *BsrGI* and *NotI*. Both the PCR amplification product and pYD2/L_C were digested with *BsrGI* and *NotI*, purified and then ligated together to yield the final vector pYD2/L_C-H_N.

For domain epitope mapping of BoNT/A antibodies, the plasmids pYD2/H_C, pYD2/L_C, pYD2/H_N (including the belt), pYD2/H_N (without the belt) and pYD2/L_C-H_N were transformed to LiAc-treated EBY100Zeo cells. Yeast cultures were then grown and induced, as described above. To quantitate binding to botulinum neurotoxin domains, ING2 that recognizes BoNT/A L_C, ING1 and 9D8 recognizing BoNT/A H_N, HuC25, AR2 and 3D12 recognizing BoNT/A1 H_C were used. Purified 3D12 and AR2 were directly labeled with Alexa-647 (Molecular

Probes, CA). Purified HuC25, ING1, and ING2 were indirectly labeled with PE-goat-anti-human IgG and 9D8 with PE-goat-anti-mouse IgG.

To measure antibody binding within the yeast surface display context, only domain displaying yeast (binding to SV5 mAb) were included in the analysis by co-staining with SV5 (Alexa-488) or SV5 (Alexa-647).

Construction and expression of a mutant BoNT/A H_C yeast displayed library

A library of H_C mutants was generated by random mutagenesis using error prone PCR, as described by Fromant and coworkers [26]. Briefly, primers Gap5 and Gap3 and Taq polymerase were used to PCR amplify H_C from the plasmid pYD2/H_C in a reaction mixture which included 0.5 mM $MnCl_2$ and an excess concentration of one of the four substrate dNTPs. The amplified mutated H_C PCR product was then gel purified using a gel extraction kit by Qiagen (Valencia, CA) and approximately 12 μg of H_C and 12 μg of *NcoI*-*NotI*-digested-pYD2 vector (3:1 insert:vector molar ratio) were used to transform LiAc-treated EBY100Zeo cells by gap repair. Transformation mixtures were cultured and subcultured in SD-CAA media. The size of the library in yeast was calculated from the number of colonies appearing on SD-CAA plates that were plated with serial dilutions of the transformation mixture. The estimated error-rate of the mutagenic library was determined by colony-PCR amplification from single colonies with primers PYDFor and GAP3Rev, followed by sequencing (Elim Biopharmaceuticals, CA) with primer PYDFor and GAP31Rev. When the OD_{600} of the subcultured library reached 1, H_C yeast surface display was induced by culturing in SG-CAA media for 48 hours at 18°C.

Selection and analysis of mutant H_C libraries by FACS

In order to maintain the library or sort output diversity, an amount of yeast at least ten times larger than the library size or the sort output from the previous round were washed and resuspended in FACS buffer (phosphate-buffered saline (pH 7.4), 0.5% bovine serum albumin).

For the first round of selection, yeast were stained with AR2 (Alexa-647), 3D12 (Alexa-647) and SV5 (Alexa-488) at 1:200 dilution (in FACS buffer) for 2 h at 4°C. All yeast displaying H_C binding AR2 and/or 3D12, regardless of display level (SV5 staining) were gated for selection on a FACSAria sorter (BD Biosciences, MD). For the second round of sorting, yeast were stained with 3D12 (Alexa-647) and AR2 (Alexa-488) and sort gates were set to collect yeast displaying H_C binding 3D12 or AR2. For the final round of sorting, induced yeast cells were incubated with AR2 (Alexa-488), 3D12 (Alexa-647) and unlabeled SV5 at 1:200 dilution (in FACS buffer) for 2 h at 4°C. Cells were then washed and incubated with the secondary antibody PE-goat-anti-mouse IgG at 1:300 dilution for 1 h at 4°C. Yeast cells were then washed and resuspended in ice-cold FACS buffer. Gates on the FACSAria were set so that only yeast displaying H_C that bound exclusively to either AR2 (Alexa-488) or to 3D12 (Alexa-647) would be selected (see Figure 3). Fluorescence compensation on FACSAria was necessary in order to subtract the inherent overlap of emission spectra that originate in the antibody PE and Alexa-488 fluorescent labels. Independent gates were set to collect separately yeast displaying H_C that were poorly displayed or had no detectable display as measured by SV5 binding.

Following the third round of selection, individual clones from the sort output were inoculated in SD-CAA and then induced in SG-CAA media, as previously described. Induced cells were washed, resuspended in FACS buffer and incubated for 2 h at room temperature with 500 pM HuC25 IgG or 500 pM 3D12 IgG, followed by 1 h incubation with SV5 (Alexa-488) IgG and APC-goat anti-human F_{AB} at 1:200 dilution at 4°C. Plasmids from yeast clones binding exclusively to HuC25 or 3D12 antibodies were recovered using a modified protocol of Qiagen (Valencia, CA) which uses acid-washed glass beads (Sigma, MO) for the efficient lysis of yeast

cells. Recovered plasmids were then transformed into chemically competent *E. coli* DH5α cells. A high copy number of these plasmids could then be recovered using a miniprep kit (Qiagen, CA) and their sequences were confirmed by DNA sequencing (Elim Biopharmaceuticals, CA) with primers PYDFor and PYDRev.

Construction and yeast display of BoNT/A H_C single alanine mutants

Genes encoding botulinum neurotoxin H_C fragments with a single alanine substitution were constructed using a one-step polymerase chain reaction (PCR). Complementary sets of primers (HCAlaFor and HCAlaRev) were designed so that they could generate a single alanine substitution at the desired amino acid position of the H_C gene fragment.

First, PYDFor and HCAlaRev (a different primer for each alanine mutation) were used to PCR amplify the 5′ end part of the H_C gene from pYD2/H_C, introducing an alanine mutation into the desired amino acid location. Similarly, PYDRev and HCAlaFor (a different primer for each alanine mutation) were used to PCR amplify the 3′ end portion of the H_C gene (Figure 4). The 5′and 3′ end PCR products were then gel-purified using a gel extraction kit (Qiagen, CA) and were used to co-transform LiAc-treated EBY100Zeo cells with *NcoI*-*NotI*-digested pYD2 vector. The pYD2-H_C (with alanine substitution) plasmids resulting from gap repair were then recovered from yeast cells, re-transformed into DH5α *E. coli* cells and their sequences were confirmed by DNA sequencing (Elim Biopharmaceuticals, CA) using PYDFor and PYDRev primers, as previously described.

Construction of BoNT/A1 H_C mutants with BoNT/A2 amino acid substitutions

Similarly to the construction of the BoNT/A1 alanine mutants, four BoNT/A1 H_C mutants were generated with BoNT/A2 substitutions at the specified amino acid locations: a) Y1117F, b) Q1254L, F1255Y, N1256D, c) I1271V, E1272G, R1273K, S1274A, d) R1294S, P1295S. The four pYD2-H_C plasmids (with the BoNT/A2 substitutions) resulting from gap-repair were recovered from yeast cells and their sequences were confirmed with PYDFor and PYDRev primers, as previously described.

Generation and purification of F_{AB} from IgG

F_{AB} fragments were prepared from purified IgG using immobilized papain (Pierce Biotechnology, IL). Briefly, IgG was concentrated to ~12 mg ml^{-1} in 20 mM phosphate, 10 mM EDTA pH 7.0, then added to an equal volume of immobilized papain resin (washed with 20mM phosphate, 10 mM EDTA, 20 mM cysteine pH 7.0) and incubated at 37°C for 16 hours. The immobilized papain was removed by centrifugation, and the digest supernatant was dialyzed against 10 mM MES pH 5.6. The F_{AB} fragment was separated from undigested IgG and F_C fragments by cation exchange chromatography (HiTrap SP HP, GE Healthcare, NJ) using a salt gradient. The purified F_{AB} was then dialyzed against PBS and stored at −80°C.

To ensure that the F_{AB} retained the expected affinity, the K_D of HuC25 and 3D12 IgG and F_{AB} fragments for yeast-displayed H_C were measured by flow cytometry. The measured K_D values for 3D12 and HuC25 IgGs (90 pM and 20 pM respectively) were comparable to the solution K_D previously measured (61 and 45 pM respectively) [22]. As expected, the equilibrium K_D of the monovalent 3D12 and HuC25 F_{AB} fragments on yeast displayed H_C, 175pM and 107 pM respectively, were also comparable to the solution K_D but lower than the K_D values of their bivalent IgG counterparts.

Affinity (K_D) measurement of F_{AB} fragments on wild type H_C and alanine mutants

The dissociation equilibrium constants (K_D) of 3D12 and HuC25 F_{AB} fragments for the wild type or alanine-substituted mutants of yeast displayed H_C were measured by flow cytometry

on a LSRII flow cytometer (BD Biosciences, MD). First, EBY100Zeo yeast cultures harboring the pYD2/H_C (wild type) or the pYD2/H_C (alanine substituted) plasmids were grown and then induced as described above. Aliquots of approximately 1×10^5 induced yeast cells (i.e., ~0.005 OD_{600} ml^{-1}) were washed in FACS buffer and incubated with dilutions (ranging from 1μM-16pM) of 3D12 or HuC25 F_{AB} fragments such that the K_D would be spanned by at least 10-fold, where possible. Incubation volumes were chosen to ensure that a 10-fold molar excess of the antibody (ligand) over the displayed moiety (H_C) would be maintained. For this purpose, we assumed that ~10^5 H_C copies are displayed on the surface of a yeast cell. Incubation with 3D12 or HuC25 F_{AB} was allowed to proceed for 2 hours at room temperature. At that point, cells were washed in FACS buffer and then resuspended in secondary APC-conjugated F_{AB}-specific goat-anti-human $F_{(AB)'2}$ at 1:200 dilution in FACS buffer. To measure the K_D of 3D12 and HuC25 F_{AB} fragments within the surface display context, only the H_C displaying yeast were included in the analysis by co-staining with SV5 (Alexa-488) mAb.

Changes in free energy of binding ($\Delta\Delta G_{mut\text{-}wt}$)

For each H_C alanine mutation that significantly decreased 3D12 or HuC25 F_{AB} binding, the change of free energy ($\Delta\Delta G_{mut\text{-}wt}$) between the H_C alanine (Ala) mutant relative to that of the wild type (wt) was calculated using the following standard formula and substituting with the previously measured K_D constants:

$$\Delta\Delta G_{mut-wt} = RTln\ (K_{D,Ala} / K_{D,wt})$$

These $\Delta\Delta G_{mut\text{-}wt}$ calculations provided us with a measure of the energetic contribution of each one of the alanine-substituted amino acid residues on 3D12 or HuC25 binding, therefore indicating the position of their functional epitopes.

Competition of 3D12 F_{AB} with a synthetic peptide epitope

The synthetic peptide N-KYVDVNNVGIRGYMYLKGP-C was purchased from Genemed Synthesis (South San Francisco, CA). Serial dilutions (ranging from 1 to 300μM) of the peptide in PBS buffer solution were allowed to interact for 1h at room temperature with K_D concentration of 3D12 F_{AB}. Following incubation with the 3D12 F_{AB}, the 3D12 F_{AB}-peptide mixtures were added to 10^6 H_C-displaying EBY100Zeo (pYD2-H_C) yeast cells for 45 min at room temperature. Cells were then washed, incubated for 30 min with secondary APC-conjugated F_{AB}-specific goat-anti-human $F_{(AB)'2}$ at 1:200 dilution in FACS buffer and SV5 (Alexa-488) and analyzed by FACS.

Acknowledgements

This work was partially supported by NIAID cooperative agreement U01 AI056493 and DoD contract DAMD17-03-C-0076.

References

1. Gill DM. Bacterial toxins: a table of lethal amounts. Microbiol Rev 1982;46:86–94. [PubMed: 6806598]
2. Lacy DB, Tepp W, Cohen AC, DasGupta BR, Stevens RC. Crystal structure of botulinum neurotoxin type A and implications for toxicity. Nat Struct Biol 1998;5:898–902. [PubMed: 9783750]
3. Simpson LL. Kinetic studies on the interaction between botulinum toxin type A and the cholinergic neuromuscular junction. J Pharmacol Exp Ther 1980;212:16–21. [PubMed: 6243359]
4. Montecucco C, Schiavo G. Structure and function of tetanus and botulinum neurotoxins. Q Rev Biophys 1995;28:423–472. [PubMed: 8771234]
5. Dong M, Yeh F, Tepp WH, Dean C, Johnson EA, Janz R, Chapman ER. SV2 is the protein receptor for botulinum neurotoxin A. Science 2006;312:592–596. [PubMed: 16543415]

6. Dolly JO, Black J, Williams RS, Melling J. Acceptors for botulinum neurotoxin reside on motor nerve terminals and mediate its internalization. Nature 1984;307:457–460. [PubMed: 6694738]
7. Mahrhold S, Rummel A, Bigalke H, Davletov B, Binz T. The synaptic vesicle protein 2C mediates the uptake of botulinum neurotoxin A into phrenic nerves. FEBS Lett 2006;580:2011–2014. [PubMed: 16545378]
8. Schiavo G, Benfenati F, Poulain B, Rossetto O, Polverino de Laureto P, DasGupta BR, Montecucco C. Tetanus and botulinum-B neurotoxins block neurotransmitter release by proteolytic cleavage of synaptobrevin. Nature 1992;359:832–835. [PubMed: 1331807]
9. Schiavo G, Rossetto O, Catsicas S, Polverino de Laureto P, DasGupta BR, Benfenati F, Montecucco C. Identification of the nerve terminal targets of botulinum neurotoxin serotypes A, D, and E. J Biol Chem 1993;268:23784–23787. [PubMed: 8226912]
10. Centers for Disease Control. Handbook for Epidemiologists, Clinicians,and Laboratory Workers. Atlanta: Georgia U.S. Department of Health and Human Services, Public Health Service; 1998. Botulism in the United States, 1899–1998. downloadable at http://www.bt.cdc.gov/agent/botulism/index,asp
11. Arnon SS, Schechter R, Inglesby TV, Henderson DA, Bartlett JG, Ascher MS, Eitzen E, Fine AD, Hauer J, Layton M, Lillibridge S, Osterholm MT, et al. Botulinum toxin as a biological weapon: medical and public health management. JAMA 2001;285:1059–1070. [PubMed: 11209178]
12. United Nations Security Council. (1995). Tenth report of the executive committee of the special commision established by the secretary-general pursuant to paragraph 9 (b) (I) of security council resolution 687 (1991), and paragraph 3 of resolution 699 (1991) on the activities of the Special Commision Council, U.N.S.S/1995/1038.
13. Center for Nonproliferation Studies, Monterey Institute of International Studies. (1999). Former Soviet biological weapons facilities in Kazakhstan: past, present, and future. Bozheyeva, G., Kunakbayev, Y. & Yeleukenov, D. June 1999: 1–20. Occasional paper No.1.
14. Franz, DR.; Pitt, LM.; Clayton, MA.; Hanes, MA.; Rose, KJ. Botulinum and Tetanus Neurotoxins: Neurotransmission and Biomedical Aspects. DasGupta, BR., editor. Plenum Press; New York: 1993. p. 473-476.
15. Black RE, Gunn RA. Hypersensitivity reactions associated with botulinal antitoxin. Am J Med 1980;69:567–570. [PubMed: 7191633]
16. Amersdorfer P, Wong C, Smith T, Chen S, Deshpande S, Sheridan R, Marks JD. Genetic and immunological comparison of anti-botulinum type A antibodies from immune and non-immune human phage libraries. Vaccine 2002;20:1640–1648. [PubMed: 11858873]
17. Nowakowski A, Wang C, Powers DB, Amersdorfer P, Smith TJ, Montgomery VA, Sheridan R, Blake R, Smith LA, Marks JD. Potent neutralization of botulinum neurotoxin by recombinant oligoclonal antibody. Proc Natl Acad Sci U S A 2002;99:11346–11350. [PubMed: 12177434]
18. Swaminathan S, Eswaramoorthy S. Structural analysis of the catalytic and binding sites of Clostridium botulinum neurotoxin B. Nat Struct Biol 2000;7:693–699. [PubMed: 10932256]
19. Eswaramoorthy S, Kumaran D, Swaminathan S. Crystallographic evidence for doxorubicin binding to the receptor-binding site in Clostridium botulinum neurotoxin B. Acta Crystallogr D Biol Crystallogr 2001;57:1743–1746. [PubMed: 11679763]
20. Boder ET, Wittrup KD. Yeast surface display for screening combinatorial polypeptide libraries. Nat Biotechnol 1997;15:553–557. [PubMed: 9181578]
21. Chao G, Cochran JR, Wittrup KD. Fine epitope mapping of anti-epidermal growth factor receptor antibodies through random mutagenesis and yeast surface display. J Mol Biol 2004;342:539–550. [PubMed: 15327953]
22. Razai A, Garcia-Rodriguez C, Lou J, Geren IN, Forsyth CM, Robles Y, Tsai R, Smith TJ, Smith LA, Siegel RW, Feldhaus M, Marks JD. Molecular evolution of antibody affinity for sensitive detection of botulinum neurotoxin type A. J Mol Biol 2005;351:158–169. [PubMed: 16002090]
23. Mullaney BP, Pallavicini MG, Marks JD. Epitope mapping of neutralizing botulinum neurotoxin A antibodies by phage display. Infect Immun 2001;69:6511–6514. [PubMed: 11553596]
24. Amersdorfer P, Wong C, Chen S, Smith T, Desphande S, Sheridan R, Finnern R, Marks JD. Molecular characterization of murine humoral immune response to botulinum neurotoxin type A binding

domain as assessed using phage antibody libraries. Infect Immun 1997;65:3743–3752. [PubMed: 9284147]

25. Smith TJ, Lou J, Geren IN, Forsyth CM, Tsai R, Laporte SL, Tepp WH, Bradshaw M, Johnson EA, Smith LA, Marks JD. Sequence variation within botulinum neurotoxin serotypes impacts antibody binding and neutralization. Infect Immun 2005;73:5450–5457. [PubMed: 16113261]
26. Fromant M, Blanquet S, Plateau P. Direct random mutagenesis of gene-sized DNA fragments using polymerase chain reaction. Anal Biochem 1995;224:347–353. [PubMed: 7710092]
27. Cunningham BC, Wells JA. High-resolution epitope mapping of hGH-receptor interactions by alanine-scanning mutagenesis. Science 1989;244:1081–1085. [PubMed: 2471267]
28. Wells JA. Systematic mutational analyses of protein-protein interfaces. Methods Enzymol 1991;202:390–411. [PubMed: 1723781]
29. Nielsen UB, Adams GP, Weiner LM, Marks JD. Targeting of bivalent anti-ErbB2 diabody antibody fragments to tumor cells is independent of the intrinsic antibody affinity. Cancer Res 2000;60:6434–6440. [PubMed: 11103810]
30. Lacy DB, Stevens RC. Sequence homology and structural analysis of the Clostridial neurotxins. J Mol Biol 1999;291:1091–1104. [PubMed: 10518945]
31. Rummel A, Mahrhold S, Bigalke H, Binz T. The HCC-domain of botulinum neurotoxins A and B exhibits a singular ganglioside binding site displaying serotype specific carbohydrate interaction. Mol Microbiol 2004;51:631–643. [PubMed: 14731268]
32. Tavallaie M, Chenal A, Gillet D, Pereira Y, Manich M, Gibert M, Raffestin S, Popoff MR, Marvaud JC. Interaction between the two subdomains of the C-terminal part of the botulinum neurotoxin A is essential for the generation of protective antibodies. FEBS Lett 2004;572:299–306. [PubMed: 15304366]
33. Herreros J, Lalli G, Montecucco C, Schiavo G. Tetanus toxin fragment C binds to a protein present in neuronal cell lines and motoneurons. J Neurochem 2000;74:1941–1950. [PubMed: 10800937]
34. Frank R, Overwin H. SPOT synthesis. Epitope analysis with arrays of synthetic peptides prepared on cellulose membranes. Methods Mol Biol 1996;66:149–169. [PubMed: 8959713]
35. Christmann A, Wentzel A, Meyer C, Meyers G, Kolmar H. Epitope mapping and affinity purification of monospecific antibodies by Escherichia coli cell surface display of gene-derived random peptide libraries. J Immunol Methods 2001;257:163–173. [PubMed: 11687250]
36. Benichou S, Inchauspe G. Random fragment libraries using yeast expression plasmid. Methods Mol Biol 1996;66:241–255. [PubMed: 8959720]
37. Wang LF, Yu M. Epitope identification and discovery using phage display libraries: applications in vaccine development and diagnostics. Curr Drug Targets 2004;5:1–15. [PubMed: 14738215]
38. Mehra V, Sweetser D, Young RA. Efficient mapping of protein antigenic determinants. Proc Natl Acad Sci U S A 1986;83:7013–7017. [PubMed: 2428046]
39. Weiss GA, Watanabe CK, Zhong A, Goddard A, Sidhu SS. Rapid mapping of protein functional epitopes by combinatorial alanine scanning. Proc Natl Acad Sci U S A 2000;97:8950–8954. [PubMed: 10908667]
40. Vajdos FF, Adams CW, Breece TN, Presta LG, de Vos AM, Sidhu SS. Comprehensive functional maps of the antigen-binding site of an anti-ErbB2 antibody obtained with shotgun scanning mutagenesis. J Mol Biol 2002;320:415–428. [PubMed: 12079396]
41. Oliphant T, Engle M, Nybakken GE, Doane C, Johnson S, Huang L, Gorlatov S, Mehlhop E, Marri A, Chung KM, Ebel GD, Kramer LD, et al. Development of a humanized monoclonal antibody with therapeutic potential against West Nile virus. Nat Med 2005;11:522–530. [PubMed: 15852016]
42. Hall YH, Chaddock JA, Moulsdale HJ, Kirby ER, Alexander FC, Marks JD, Foster KA. Novel application of an in vitro technique to the detection and quantification of botulinum neurotoxin antibodies. J Immunol Methods 2004;288:55–60. [PubMed: 15183085]
43. Montero-Julian FA, Klein B, Gautherot E, Brailly H. Pharmacokinetic study of anti-interleukin-6 (IL-6) therapy with monoclonal antibodies: enhancement of IL-6 clearance by cocktails of anti-IL-6 antibodies. Blood 1995;85:917–924. [PubMed: 7849313]
44. Clayton MA, Clayton JM, Brown DR, Middlebrook JL. Protective vaccination with a recombinant fragment of Clostridium botulinum neurotoxin serotype A expressed from a synthetic gene in Escherichia coli. Infect Immun 1995;63:2738–2742. [PubMed: 7790092]

45. Potter KJ, Zhang W, Smith LA, Meagher MM. Production and purification of the heavy chain fragment C of botulinum neurotoxin, serotype A, expressed in the methylotrophic yeast Pichia pastoris. Protein Expr Purif 2000;19:393–402. [PubMed: 10910730]

46. Smith LA, Jensen MJ, Montgomery VA, Brown DR, Ahmed SA, Smith TJ. Roads from vaccines to therapies. Mov Disord 19 Suppl 2004;8:S48–52.

47. Ahmed SA, Smith LA. Light chain of botulinum A neurotoxin expressed as an inclusion body from a synthetic gene is catalytically and functionally active. J Protein Chem 2000;19:475–487. [PubMed: 11195972]

48. Jensen MJ, Smith TJ, Ahmed SA, Smith LA. Expression, purification, and efficacy of the type A botulinum neurotoxin catalytic domain fused to two translocation domain variants. Toxicon 2003;41:691–701. [PubMed: 12727273]

49. Gietz RD, Schiestl RH. Applications of high efficiency lithium acetate transformation of intact yeast cells using single-stranded nucleic acids as carrier. Yeast 1991;7:253–263. [PubMed: 1882550]

50. Feldhaus MJ, Siegel RW, Opresko LK, Coleman JR, Feldhaus JM, Yeung YA, Cochran JR, Heinzelman P, Colby D, Swers J, Graff C, Wiley HS, et al. Flow-cytometric isolation of human antibodies from a nonimmune Saccharomyces cerevisiae surface display library. Nat Biotechnol 2003;21:163–170. [PubMed: 12536217]

Abbreviations used

APC
: allophycocyanin

BoNT/A
: botulinum neurotoxin serotype A

BoNT/A H_C
: botulinum neurotoxin serotype A binding domain

BoNT/A H_N
: botulinum neurotoxin serotype A translocation domain

BoNT/A L_C
: botulinum neurotoxin serotype A light chain

F_{AB}
: antibody binding fragment

FACS
: fluorescence activated cell sorting

Fc
: antibody crystalizable fragment

IgG
: immunoglobulin G

K_D
: dissociation equilibrium constant

MAb
: monoclonal antibody

MFI
: mean fluorescence intensity

PCR

polymerase chain reaction

PE

phycoerythrin

scFv

single-chain variable fragment

SD-CAA

selective growth dextrose Casamino acids media

SG-CAA

selective growth galactose Casamino acids media

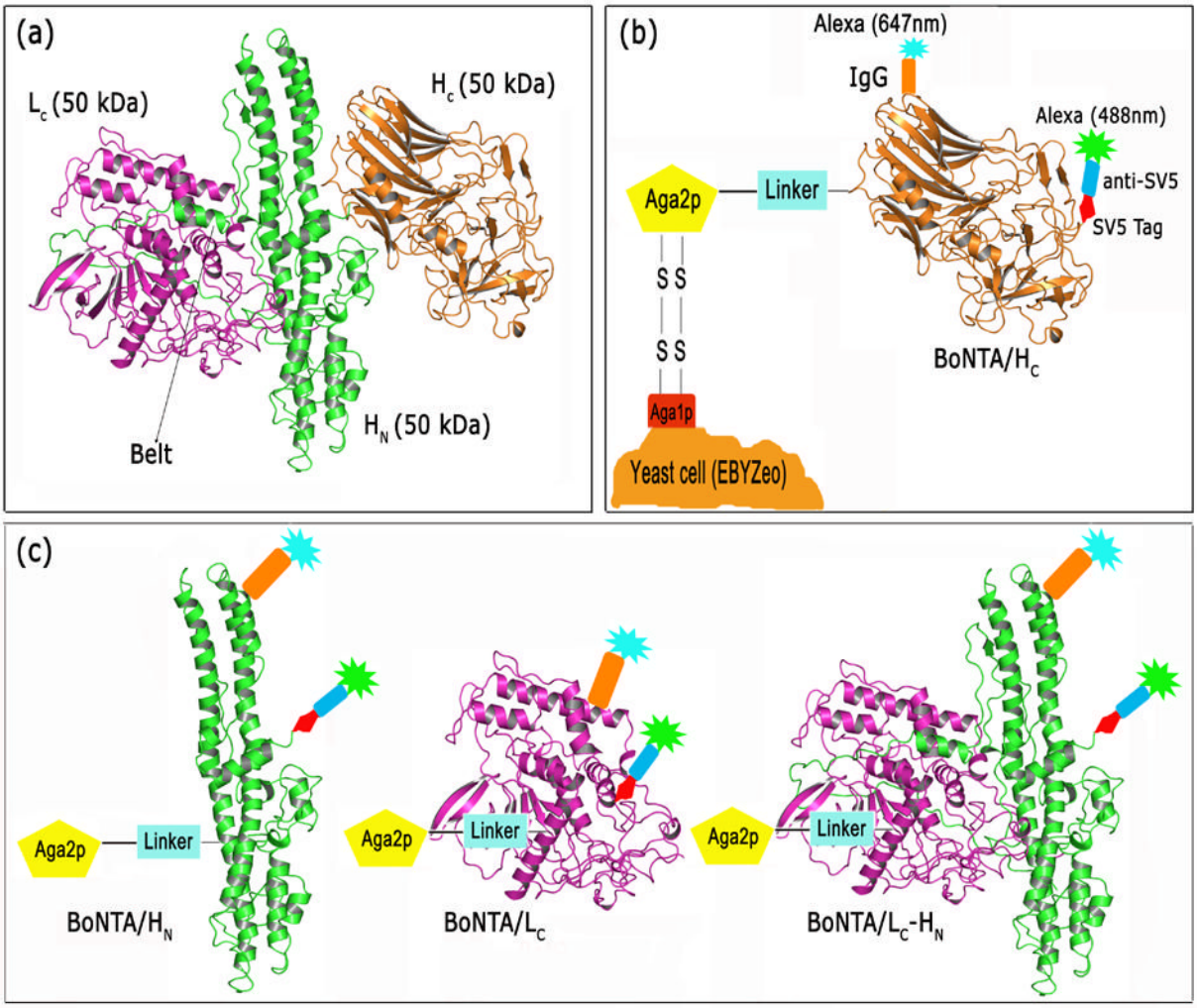

Figure 1. Yeast surface display of BoNT/A domains

(a) Ribbon cartoon of the X-ray crystal structure of BoNT/A secondary structure (PDB accession name, 3BTA) showing catalytic light chain (L_C, magenta), binding (H_C, orange) and translocation (H_N, green) domains 2. The belt region of H_N, which wraps around the L_C, is indicated. (b) Schematic representation of yeast displayed H_C, fused to the yeast protein Aga2p via a flexible $(Gly_4Ser)_3$ linker. The level of yeast display is quantitated via direct or indirect (not shown) fluorescent labeling of an SV5 epitope-tag binding monoclonal antibody. A fluorescent labeled BoNT/A-specific IgG is used to independently verify display. (c) Yeast display of BoNT/A H_N, BoNT/A L_C, and BoNT/A L_C-H_N. SV5 epitope tag and domain specific mAbs are shown bound to their respective domains.

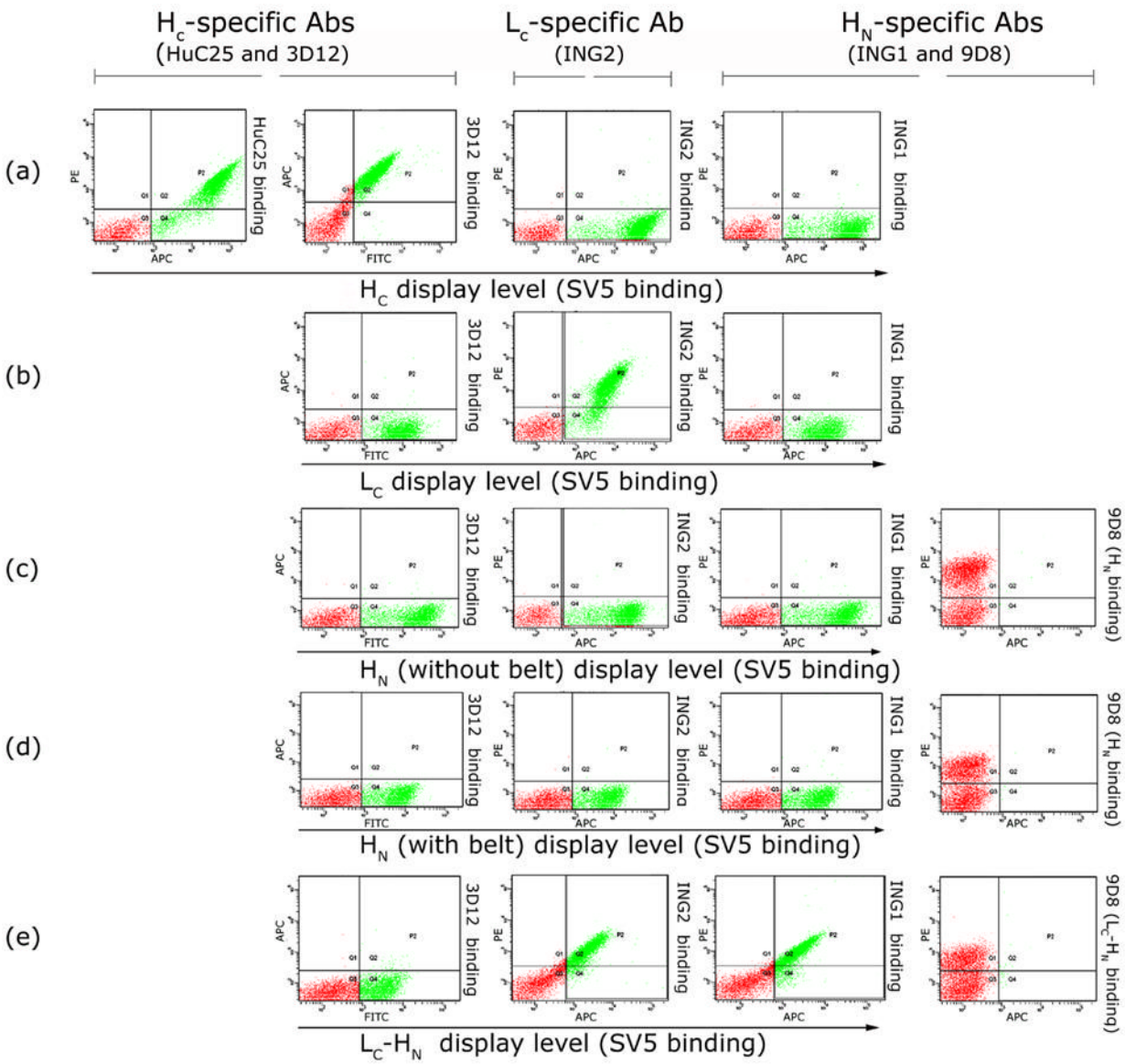

Figure 2. Yeast display of BoNT/A domains and mapping of BoNT/A monoclonal antibodies by flow cytometry

Specific binding to (a) yeast-displayed H_C by human mAbs HuC25 and 3D12; (b) yeast-displayed L_C by human mAb ING2; (c) and (d) yeast-displayed H_N (with (c) or without (d) the belt region) by murine mAb 9D8, and (e) yeast-displayed L_C-H_N by mAbs ING2, 9D8 and ING1. All domains are well displayed as indicated by a greater than 2 log shift with anti-SV5. All domains are bound only by domain specific mAbs, with no binding of mAbs specific to other domains.

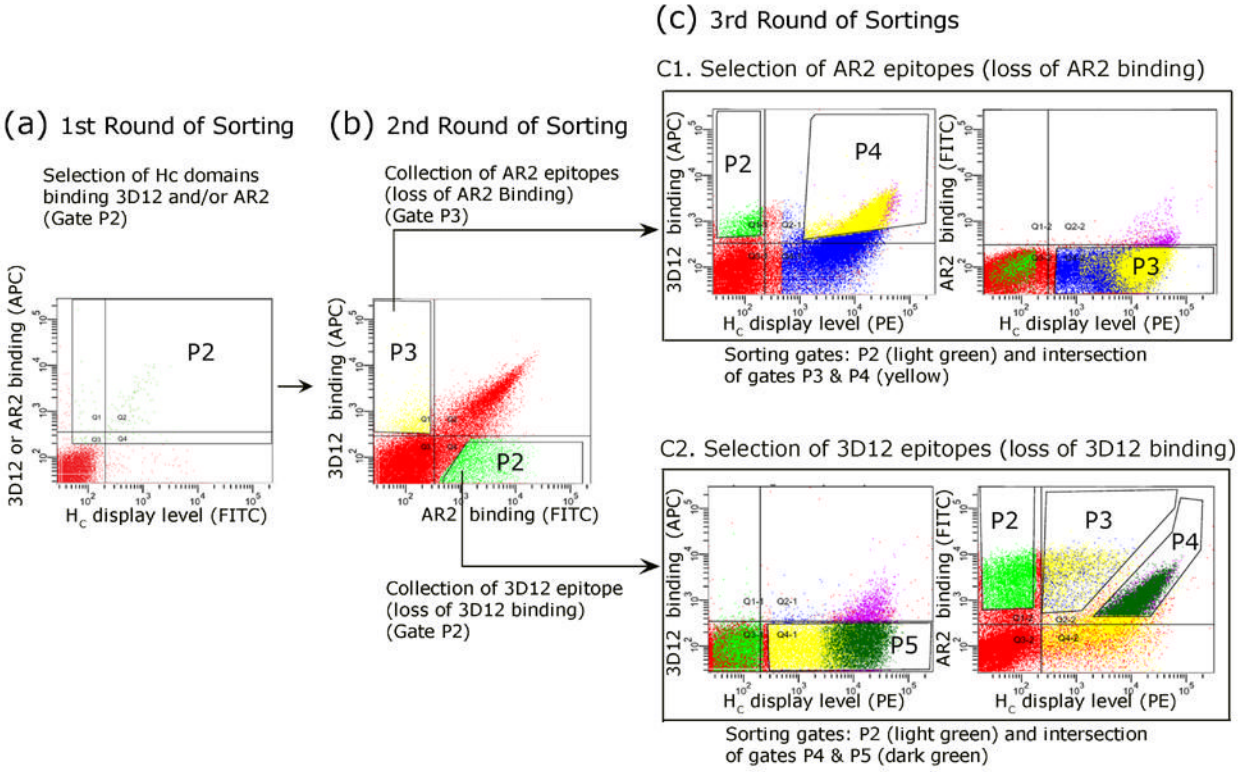

Figure 3. Selection of yeast-displayed BoNT/A H_C with mutations that knocked out mAb binding

BoNT/A H_C clones with mutations knocking out binding to mAb 3D12 or mAb AR2 were selected from a library of yeast displayed BoNT/A H_C mutants using FACS. The first round of sorting (a) was designed to merely enrich for yeast displaying BoNT/A H_C capable of binding 3D12 and/or AR2 in preparation for subsequent rounds of sorting. This was accomplished by simultaneously staining yeast with mAbs 3D12 and AR2 labeled with Alexa-647 and SV5-Alexa-488. Yeast displayed BoNT/A H_C that were bound by mAbs 3D12 and/or AR2 (APC channel) were gated for selection (gate P2), regardless of display level (SV5-Alexa-488 (FITC) staining). The second round of sorting (b) was designed to isolate yeast displayed BoNT/A H_C that contained mutations which resulted in loss of binding to one of the two mAbs but which retained binding to the other BoNT/A mAb. Requiring binding to the second BoNT/A mAb helped ensure that the selected domains were properly folded. This was accomplished by staining yeast with 3D12-Alexa-647 and AR2-Alexa-488. Yeast that lost binding to AR2 (gate P3), or that had lost binding to 3D12 (gate P2) were separately gated and sorted. The final round of sorting (c) was designed to complete the isolation of yeast displayed BoNT/A H_C which had mutations that resulted in the loss of binding to one of the two BoNT/A mAbs but which retained binding to the other BoNT/A mAb. For the final round of sorting, yeast from second round gates P2 and P3 were stained in separate reactions with 3D12-Alexa-647 and AR2-Alexa-488 mAbs and anti-SV5-epitope tag mAb followed by anti-mouse PE. For sorting of yeast from the second round gate P3 selected for loss of binding to AR2, yeast without binding to AR2 (gate P3, blue dots) but with retained binding to 3D12 (gate P4, purple dots) were selected by intersecting the P3 and P4 gates (yellow dots) and collecting only those yeast in both gates (c, top panels). Yeast with the same phenotype, but without SV5 binding (truncation mutants, gate P2, green dots) were also sorted. For the final round of sorting of yeast from the second round gate P2 selected for loss of binding to 3D12, yeast without binding to 3D12 (gate P5, yellow dots) but with retained binding to AR2 (gate P4, purple dots) were selected by intersecting the P5 and P4 gates (dark green dots) and collecting only those

yeast in both gates (c, bottom panels). Yeast with the same phenotype, but without SV5 binding (truncation mutants, gate P2, green dots) were also sorted.

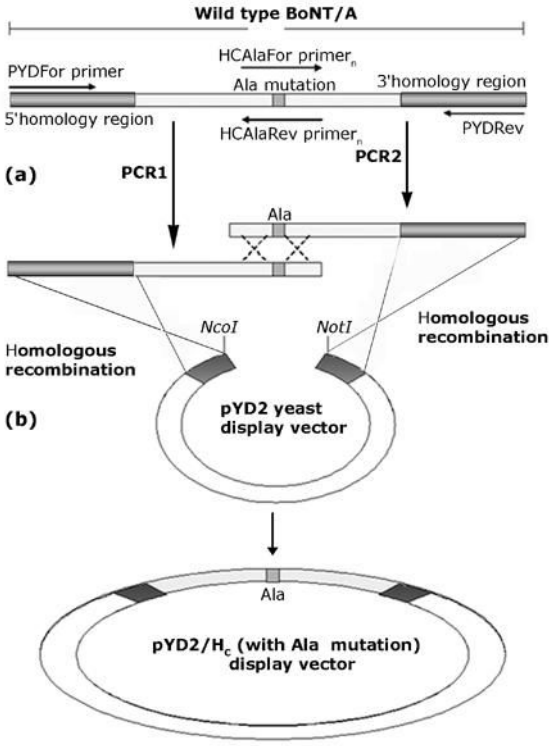

Figure 4. Generation of single alanine H_C mutants by yeast gap repair

(a) The 5′ and 3′ ends of the H_C gene were PCR amplified from wild type H_C, replacing an H_C amino acid residue with an alanine. Outside primers PYDFor, PYDRev and inside alanine-introducing sets of primers $HCAlaFor_n$ and $HCAlaRev_n$ were used for PCR and introduction of the alanine mutation. (b) The PCR amplification products were then cotransformed with the *NcoI-NotI* digested display vector pYD2 into yeast to form the desired H_C single alanine mutants in pYD2 by gap repair homologous recombination.

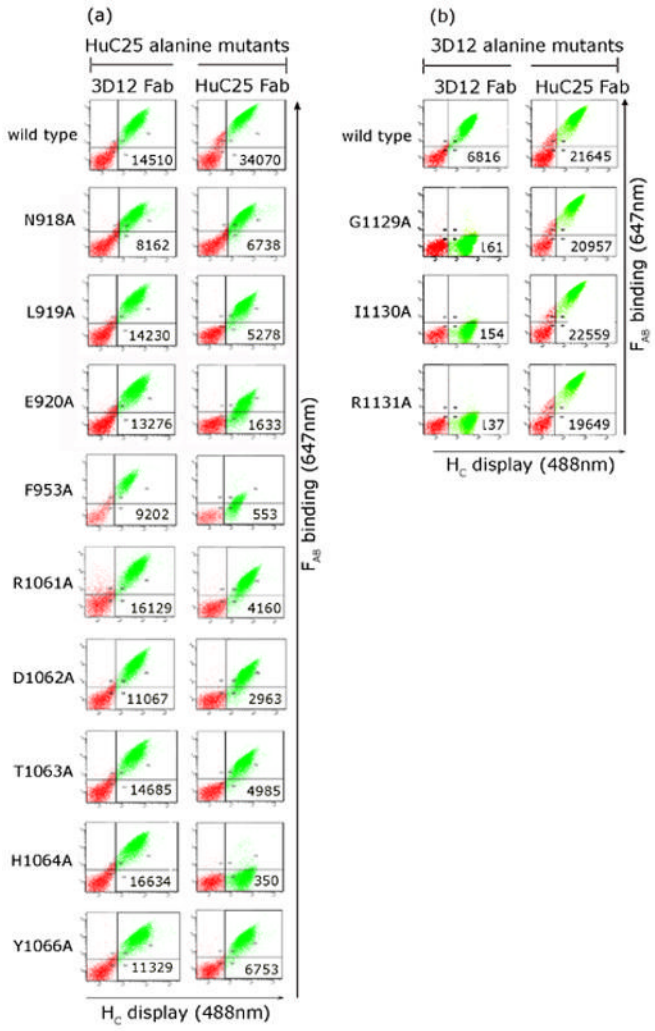

Figure 5. Binding of HuC25 and 3D12 F_{AB} fragments to yeast displayed BoNT/A H_C alanine mutants

Antibody binding to yeast displayed H_C was quantitated on a flow cytometer by co-staining with anti-SV5 (Alexa-488) and F_{ABs} HuC25 and 3D12 followed by F_{AB}-specific-APC (647 nm) labeled antisera. Mean fluorescence intensity (MFI) values for F_{AB} binding are shown. Comparison of the MFI for wildtype binding and mutant binding of HuC25 vs 3D12 F_{AB} identified alanine mutations with reduced affinity.

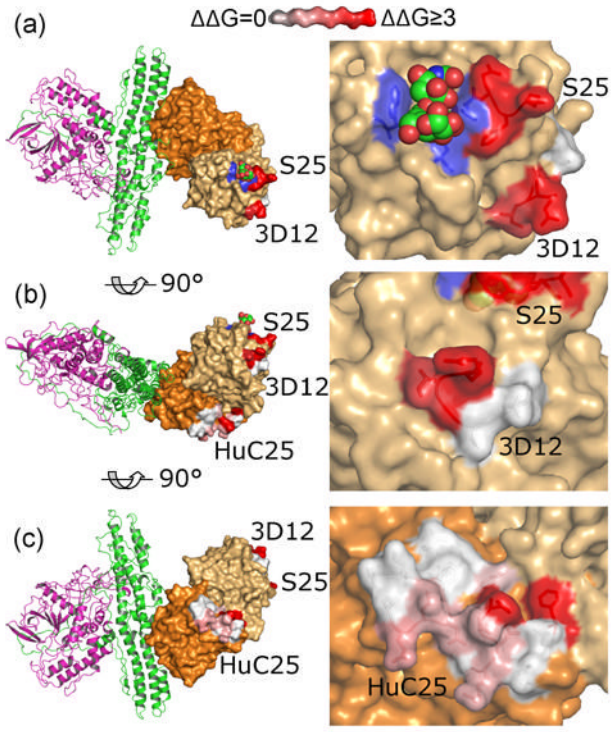

Figure 6. Model of the functional binding epitopes of neutralizing BoNT/A mAbs

The epitopes of S25 (top panels), 3D12 (middle panels) and HuC25 (bottom panels) are shown, with the ΔΔG of important toxin side chain interactions colored red-white as indicated. The putative sialoganglioside contacting residues on H_{CC} are colored blue, and the sialoganglioside is shown modeled as spheres, near the S25 epitope. H_{CC}, space filling light orange; H_{CN}, space filling dark orange, H_N, green, L_C, magenta. Molecular models were constructed using Pymol software (DeLano Scientific, LLC), using the coordinates of BoNT/A (3BTA) from the Protein Data Bank.

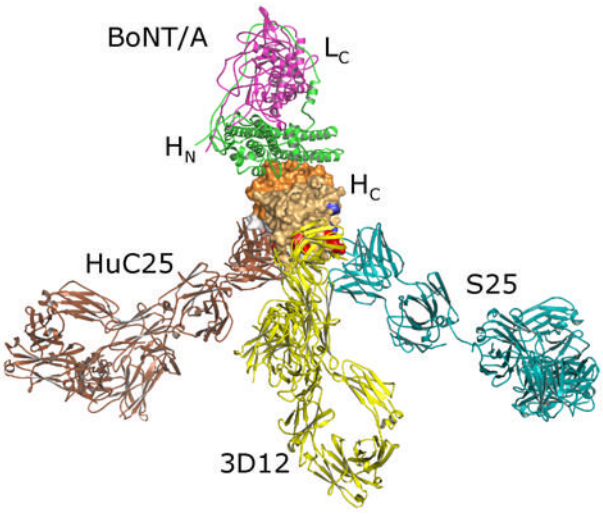

Figure 7. Model of the binding of three neutralizing mAbs to BoNT/A

The binding of S25, 3D12, and HuC25 IgG to their epitopes on BoNT/A were modeled using the coordinates of BoNT/A (3BTA) and three copies of the coordinates of an arbitrary human IgG (1HZH) using Pymol software (DeLano Scientific, LLC). The model indicates that all three mAbs could bind simultaneously, creating a large tripod shaped immune complex.

Table 1

Monoclonal antibodies mapped using surface displayed BoNT/A domains.

Antibody	BoNT/A K_D (M)	Domain specificity	In vitro neutralization (fold over control)
HuC25	4.5×10^{-11}	H_C	6.82*
3D12	6.1×10^{-11}	H_C	3.02
S25	1.7×10^{-9}	H_C	1.85
9D8	1.2×10^{-9}	H_N	ND
ING2	9.6×10^{-12}	L_C	ND
ING1	3.1×10^{-10}	L_C-H_N	ND

Solution K_D of HuC25, 3D12, ING1, and ING2 were measured in a flow fluorimeter (KinExA) (ref. 22 and unpublished data). K_D of S25 and 9D8 were measured using surface plasmon resonance (BIAcore) [25]. In vitro neutralization was determined as time to 50% neuroparalysis in the mouse hemidiaphragm assay and is expressed as fold over control [17].

*In vitro neutralization data for C25, murine precursor of humanized C25, HuC25.

Table 2

Binding of BoNT/A H_C alanine mutants to HuC25 or 3D12 F_{AB} fragments.

BoNT/A H_C mutant	HuC25 F_{AB} binding	BoNT/A H_C mutant	3D12 F_{AB} binding
S896A	++++	N1126A	++++
K897A	++++	N1127A	++++
N899A	++++	V1128A	++++
I900A	++++	G1129A	−
G901A	+++	I1130A	−
S902A	++++	R1131A	−
K903A	+++	K1187A	++++
N905A	++++		
Q915A	++++		
F917A	++++		
N918A	++		
L919A	++		
E920A	−		
S921A	++++		
E925A	++++		
I927A	++++		
K929A	++++		
N930A	++++		
F953A	−		
N954A	++++		
I956A	++++		
C1060A	++++		
R1061A	+		
D1062A	+		
T1063A	+		
H1064A	−		
Y1066A	++		
*H_{CN} (876-1092)	++++		

++++ binding of Ala mutant similar to wild-type; −, complete loss of binding;

*Deletion mutant of H_C, lacking the C-terminus portion (amino acids 1093–1296) of the domain.

Table 3

Affinities and ΔΔG of alanine-substituted BoNT/A H_C mutants.

BoNT/A H_C mutant	**HuC25 $F_{AB}K_D$ (M)**	**$\Delta\Delta G_{mut\text{-}wt}$ kcal/mol**
wt	1.07×10^{-10}	-
N918A	6.70×10^{-10}	0.9
L919A	7.44×10^{-10}	**1**
E920A	1.31×10^{-9}	**1.3**
F953A	2.15×10^{-8}	**3**
R1061A	7.51×10^{-10}	**1**
D1062A	6.06×10^{-10}	0.9
T1063A	6.42×10^{-10}	0.9
H1064A	1.35×10^{-5}	**6.8**
Y1066A	4.27×10^{-10}	0.7
BoNT/A H_C mutant	**3D12 F_{AB} K_D (M)**	**$\Delta\Delta G_{mut\text{-}wt}$ kcal/mol**
Wt	1.75×10^{-10}	-
G1129A	1.84×10^{-5}	**6.8**
I1130A	7.35×10^{-9}	**2.2**
R1131A	1.00×10^{-5}	**6.5**

The dissociation equilibrium constant (K_D) for HuC25 (or 3D12) F_{AB} was calculated for each alanine mutant. The difference in binding free energy ($\Delta\Delta G_{ala\text{-}wt}$) between the alanine-substituted and wild type (wt) H_C was calculated according to the formula $\Delta\Delta G = RT\ln(K_{D,Ala}/K_{D,wt})$ (*Materials and Methods*). Mutants in bold have $\Delta\Delta G_{mut\text{-}wt} \geq 1$.